

# Enhanced Emotional and Speed Deviation Control of Synchronous Reluctance Motor Drives

Ehsan Daryabeigi, Ahmad Mirzaei, Member, IEEE, Hossein AbootorabiZarchi, Sadegh Vaez-Zadeh, Senior Member, IEEE

**Abstract**—This paper proposes an enhanced brain emotional learning-based intelligent controller (BELBIC) for synchronous reluctance motor (SynRM) drives. The controller is based on an emotional learning and decision making mechanism in the brain via emotional cues and sensory inputs. Furthermore, the enhanced controller improves learning process in the amygdala to avoid internal instability. In spite of the development for interior-stability, the proposed controller could keep its ability to deal with challenges related to SynRM drives. The proposed controller is also contributed with a speed deviation control. The new deviation controller is based on model, but parameter-free. The updated system is implemented in real-time by a PC-based three-phase 370 W laboratory SynRM. The PI controllers used in a standard rotor field-oriented control structure are replaced with those of the proposed method. The speed and d-axis stator current references are accurately tracked. The achieved performances by the proposed controllers are compared with those of optimized conventional PI controller in different situations. Considering the results, the enhanced system shows superiority over the traditional system in terms of fast dynamics, easy tuning and robustness against disturbances and parameter variations.

**Index Terms**—Emotional controller, deviation control, motor speed control, synchronous reluctance motor.

## I. INTRODUCTION

IN recent years, the synchronous reluctance motor (SynRM) has received much attention for many applications due to its low temperature, simple and rugged rotor construction [1], [2]. Moreover, the development of vector control technique has made it possible to achieve an AC electrical drive having high dynamic responses [3], [4]. The vector control methodology of synchronous reluctance motor has been improved to obtain optimum operation at maximum torque per stator current and voltage, high efficiency and high power factor [3]. These approaches have been usually implemented with conventional

controller such as PI one [3]. Some disadvantages of the controllers, consisting of controller tuning and dependency on parameter and operation point variations, have been overcome by some nonlinear methods like variable structure control (VSC) [5], [6].

By knowing the boundaries of the system and grouped uncertainties, some challenging uncertainties including parameter variations and disturbances can be rejected by VSC. However, specific and reliable system uncertainty boundaries are difficult to obtain for practical applications. Using high gain control to improve disturbance rejection has been proposed in multi-segment sliding mode control [6]. In addition, there are predictive methods, which are usually based on a machine model. However, it is difficult to develop mathematical models of the system accurately because of unknown and unavoidable parameter variations [7], and to deal with the matter, parameter estimation methods are employed, which are usually either time consuming or computational intensive [8]. In another approach, some model free control methods have been proposed based on predictive process [9]. In [9], although a model free predictive current control is proposed to deal with tracking current references, torque or speed control is not discussed. Albeit various advanced control methods have been proposed to deal with challenges of the controllers in torque control mode, using conventional speed controllers are common [10].

Moreover, by appearance of intelligent controllers, motor drives have enjoyed some advantages in terms of fast dynamics, adaptation, self-tuning, or even auto learning [11], [12]-[17]. Notwithstanding the versatility of the intelligent systems, many of the practical applications require large computational burden to handle the complexity and real-time constraints of these systems [12]. To answer to the drawbacks, Brain Emotional Learning based on intelligent controller (BELBIC) has been proposed by C. Lucas for control applications [13]. In recent years, BELBIC has been developed and used with minimal modifications in control devices for different industrial applications [14-17].

For electrical drive control applications [18], the conventional BELBIC is represented by Rahman et al. [19]. The speed control of non-linear interior type permanent magnet synchronous motors (IPMSMs) using the BELBIC method is compared with a PID controller in terms of dynamic responses and accuracy. Moreover, a comparative study is done in [20] for IPMSM drives based on BELBIC, fuzzy

Manuscript received October 5, 2017; revised August 18, 2018; accepted September 26, 2018. (Corresponding author: Ahmad Mirzaei)

E. Daryabeigi is with the Department of Electrical Engineering, Faculty of Azadi, Yazd University, Yazd, Iran (e-mail: e.daryabeigi@gmail.com).

A. Mirzaei is with the Department of Electrical Engineering, Faculty of Engineering, Yazd University, Yazd, Iran (e-mail: mirzaei@yazd.ac.ir).

H. AbootorabiZarchi is with the Department of Electrical Engineering, Faculty of Engineering, Ferdowsi University of Mashhad, Mashhad, Iran (e-mail: abootorabi@um.ac.ir).

S. Vaez-Zadeh is with the School of Electrical and Computer Engineering and the Center of Excellence on Applied Electromagnetic Systems, College of Engineering, University of Tehran, Tehran, Iran (e-mail: vaezs@ut.ac.ir).

controller, and optimal PI controller. Furthermore, in [20] some of the control strategies such as; Maximum Torque per Ampere (MTPA) control and flux weakening (FW) control are successfully applied. In [21] a speed controller is implemented for a SynRM by using the conventional BELBIC, which excludes a detailed study of the motor drive performance and the controller drawbacks. In addition, an improved SynRM drive system based on emotional controller and MTPA strategy was presented [4]. The results show a superiority of the proposed controller over an optimal PI controller. Notwithstanding all the reported benefits, the internal instability attributed to the controller in a long run time, has not been considered, [14]. In [22] an improved BELBIC with integral anti-wind up (IAW) is introduced for this problem. Although the solution avoids increasing integral value, it causes the learning process faced with tribulations because it removes learned data when reaching saturation level of the integral. In another attempt [23], a self-tuning BELBIC based on fuzzy inference is designed to tune online reward function. Although interior stability is claimed, amygdala is still suffered from increasing learning weight during the variable operating conditions.

In this paper, an improved version of the BELBIC is presented to avoid the internal instability, which in fact occurs by increasing the amygdala learning weights. Thereby, using the proposed approach not only the emotional controllers have more effective operation but also enjoy a more reliable role in comparison with the past. Despite keeping simplicity, the control is achieved by quick auto learning, proper tracking of references adaptively, and independence of system parameters variation, which results in performance improvement. In fact, the proposed version of BELBIC not only keeps the previous advantages but also rejects probability of interior-instability.

Furthermore, PI speed regulator is replaced by a deviation format equation. Deviation models are usually used to facilitate our understanding of dynamic variations in general [24]. Also, this technique is employed for drive applications to achieve control laws such as combined control (CC) [25], or system analysis [26], [27]. Normalized version of the approach is proposed as speed deviation controller (SDC) and torque deviation controller (TDC), respectively. In the present case there is no need for PI calibration and the dynamic response of closed-loop control is invariant with the torque and speed operating point (whereas PI regulators would require gain adaptation throughout the torque-speed domain) [4]. In fact, unlike other drive systems based on the conventional PI controllers, the proposed technique based on SDC-BELBIC enjoys auto learning, parameter-free and the controller coefficients are adaptive, which facilitates FOC control for any electric drive in general.

In this paper, the conventional and deviation SynRM models in the rotor-oriented reference frame are given in section II. In section III, the mathematical model of the novel intelligent controller based on developed limbic system is presented. A block diagram of the proposed system is explained in section IV. Hardware implementation is presented in section V, and the experimental and simulation

results are presented and discussed in section VI. Finally, the concluding part of the paper is presented in section VII.

## II. SYNRM MODEL

In the synchronously rotating reference frame, the d-q axis equations for the SynRM, including iron losses, could be described in the rotor reference frame as [28]:

$$v_{ds} = (R_s \cdot i_{ds} + pL'_d) i_{dT} - \omega_{er} \cdot i_{qT}, \quad (1)$$

$$v_{qs} = (R_s \cdot i_{qs} + pL'_q) i_{qT} + \omega_{er} \cdot i_{dT}, \quad (2)$$

$$L'_d = \left(1 + \frac{R_s}{R_i}\right) L_d, \quad L'_q = \left(1 + \frac{R_s}{R_i}\right) L_q, \quad (3)$$

where  $p$  indicates differential operator,  $v_{ds}$  and  $v_{qs}$  are stator voltages,  $i_{dT}$  and  $i_{qT}$  are torque-producing current components,  $L_d$  and  $L_q$  are stator inductances, which are all in  $d$ - and  $q$ -axis rotor reference frame.  $R_i$  and  $R_s$  are iron losses and stator resistances respectively,  $\omega_{er}$  is the rotor electrical angular velocity. The electromagnetic torque could be given as [28]:

$$T_e = K_T i_{dT} i_{qT}, \quad (4)$$

where  $K_T = \frac{3P}{4} \cdot (L_d - L_q)$  is the torque constant and  $P$  denote the number of poles. The motor torque could be controlled by  $q$ -axis current  $i_{qT}$ , while the  $d$ -axis current  $i_{dT}$  is assumed constant. In addition, the electromagnetic torque could be rewritten as follows:

$$T_e = \frac{3P}{8L_d L_q} \left[ \lambda_s^2 (L_d - L_q) \sin 2\delta \right] \quad (5)$$

where “ $\lambda_s$ ” and “ $\delta$ ” are stator flux linkage and load angle, respectively.

A deviation transfer can be generally achieved by differentiating a dynamic equation. After that, differential operator is changed to deviation operator “ $\Delta$ ”, as follows:

$$z = f(x, y) \xrightarrow{\partial} dz = F(x, dx, y, dy) \xrightarrow{d \rightarrow \Delta} \Delta z = F(x, \Delta x, y, \Delta y), \quad (6)$$

where, “ $x$ ”, “ $y$ ”, and “ $z$ ”, are typical independent and dependent variables, respectively. Also, “ $f$ ”, “ $F$ ” are functions based on the variables. Here, “ $\Delta$ ”, as deviation operator, denotes a small deviation of the respective variable from the operating point. So, the torque (5) is transferred into a deviation form as:

$$\Delta T_e = \frac{3P}{4L_d L_q} \left[ \lambda_s^2 (L_d - L_q) \sin 2\delta \right] \left( \frac{\Delta \lambda_s}{\lambda_s} + \cot 2\delta \Delta \delta \right). \quad (7)$$

Although in [29] nominal values are proposed for

normalizing equations, it can't guarantee parameter independency when parameter variation considered. Hence, to get rid of parameter dependency in (7), it is divided by actual torque (5). Normalized version of the deviation equation (7) is achieved, as:

$$\Delta T_{en} = 2\Delta\lambda_{sn} + 2 \cot 2\delta\Delta\delta. \quad (8)$$

In addition, torque deviation can be rewritten by considering (4) as:

$$\Delta T_{en} = \Delta i_{dTn} + \Delta i_{qTn}, \quad (9)$$

where all the elements with index “ $n$ ” are normalized values. The achieved deviations (8)-(9) represent dynamic free-parameter equations, which can be employed in control system design and analysis.

### III. LIMBIC SYSTEM MODEL

The main aim of the work is to present a structural model based on the limbic system of mammalian brain where emotional learning is done, for decision making and control applications. A conventional model of the emotional system is shown in Fig. 1. Here, it is presented conventional emotional model with minimum explanation since precise explanation is available in many literatures such as [4]. Consequently, BELBIC model can be summarized as:

$$E = A + A_{th} - O, \quad (10)$$

where  $E$ ,  $A$ ,  $A_{th}$ , and  $O$  are model output, the first and second outputs of Amygdala, and orbitofrontal output, respectively. The outputs of the mentioned internal areas could be computed as follows:

$$A_{th} = V_{th}S_{th}, \quad (11)$$

$$A = S_c V, \quad (12)$$

$$O = (S_c + S_{th})W, \quad (13)$$

$$S_c = S \otimes e^{-kt}, \quad (14)$$

where  $V$  and  $W$  are weights of the amygdala and orbitofrontal connections,  $S$ ,  $S_c$ ,  $t$ , and  $k$  are sensory input, sensory-cortex output, time, and time constant respectively [4]. Deviation of  $V$  and  $W$  can be calculated as:

$$\Delta V = \alpha \left( \max(0, S_c (R - A)) \right), \quad (15)$$

$$V(t) = \int_0^t \Delta V dt + V(0),$$

$$\Delta V_{th} = \alpha \left( \max(0, S_{th} (R - A_{th})) \right), \quad (16)$$

$$V_{th}(t) = \int_0^t \Delta V_{th} dt + V_{th}(0).$$

Likewise, the output “ $E$ ” is obtained by subtracting output “ $A$ ” from inhibitory output “ $O$ ” as:

$$E' = A - O, \quad (17)$$

$$\Delta W = \beta \left( S_c (E' - R) \right), \quad (18)$$

$$W = \int_0^t \Delta W dt + W(0),$$

where  $\alpha$  and  $\beta$  are the learning steps in the amygdala and orbitofrontal cortex, respectively. Also,  $R$  is the value of emotional cue function at each time. The learning rule of the amygdala is given in (16), which cannot decrease. It means that it does not forget information in the amygdala. Whereas, idiomatically inhibiting (forgetting) is the duty of orbitofrontal cortex (13). Eventually, model output is obtained from (10).

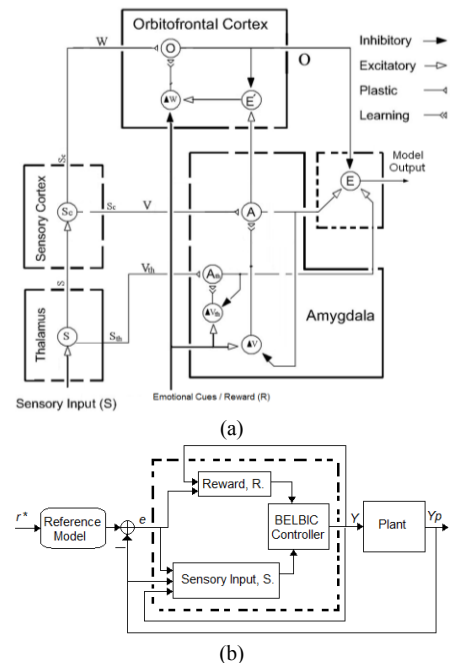


Fig. 1. a) Emotional system, Graphical depiction of the BELBIC [4]. b) General control system configuration by using the emotional controller,

If BELBIC output (10) is rewritten with considering relationships (11)-(13), the equation can be presented as follows:

$$E = A + A_{th} - O$$

$$= S_c V + S_{th} V_{th} - (S_c + S_{th})W$$

$$= (V - W)S_c + (V_{th} - W)S_{th}, \quad (19)$$

$$V_2 = V - W = \int_0^t (\Delta V - \Delta W) dt + V(0) - W(0),$$

$$V_{th2} = V_{th} - W = \int_0^t (\Delta V_{th} - \Delta W) dt + V_{th}(0) - W(0).$$

As a conclusion of the above relationships can be given as:

$$E = V_2 S_c + V_{th2} S_{th}, \quad (20)$$

where  $V_2$  and  $V_{th2}$  are named as new learning weights, which used instead of the amygdala weights (15) and (16), so that the new functions ( $V_2$  &  $V_{th2}$ ) can be increased/decreased in contrast to the primary ones (15 & 16) that only can be increased because of applying a maximum term. The problem

of increasing the amygdala learning weights until reaching saturation level of related integrals, which may occur during learning process in the amygdala, is resolved by using both the new functions. On the other words, in the proposed functions, both variations of the amygdala weights decrease by applying the orbitofrontal learning (19) before charging their integrals. Fig. 2(a) shows these signals, so that  $V_2$  &  $V_{th2}$  can be decreased/increased; on the contrary,  $V$  and  $V_{th}$  signals only can be increased, as shown in Fig. 2(b). This matter can come instability at a long operation in the conventional system. In the proposed solution, not only any learned data (information) is not lost but also it avoids unpermitted increase in the amygdala.

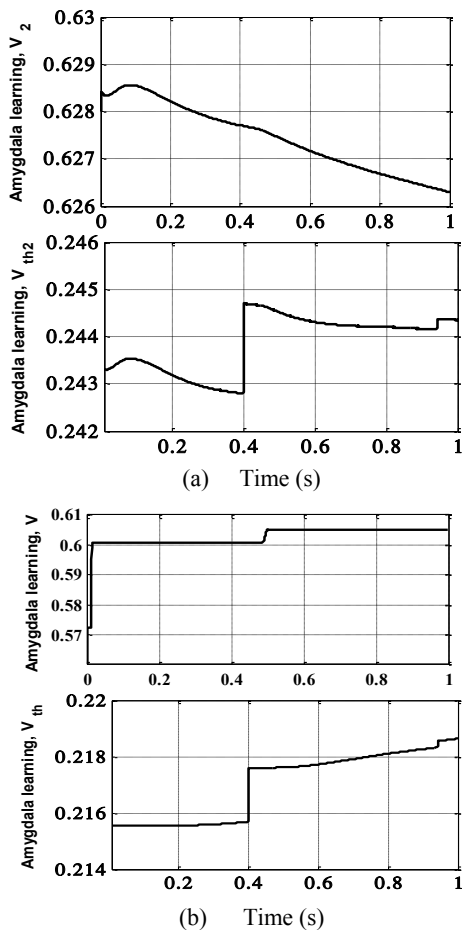


Fig. 2. The amygdala learning weights, a) proposed functions ( $V_2$  &  $V_{th2}$ ), b) primary functions ( $V$  &  $V_{th}$ ).

Fig.1(b) shows the BELBIC controller configuration. The used functions in emotional cue  $R$  and sensory input  $S$  blocks can be given by the following relations:

$$R = f(e, y, y_p), \quad (21)$$

$$S = g(e, y, y_p). \quad (22)$$

In this research, the functions  $f$  and  $g$  are given by relations:

$$g = k_1 e + k_2 \int edt, \quad (23)$$

$$g_{th} = k_1 e \cdot \left| \int edt \right|, \quad (23)$$

$$f = K_1 |e| + K_2 |e \cdot y| + 0.5 \max(|y_p| - y_{Max}, 0), \quad (24)$$

where  $e$ ,  $y$ ,  $y_p$  and  $y_{Max}$  are system error, controller output, system output and maximum output, respectively as shown in Fig.1(b).

The terms  $k_1 - k_2$ , and  $K_1 - K_2$  are gains, which tuned for designing a suitable controller. Initial values including  $V(0)$ ,  $W(0)$ ,  $\alpha$  and  $\beta$  should be chosen by trial and error. Moreover, functions “ $R$ ” and “ $S$ ” are selected for emotional signal generation.

In this proposed controller, learning process of the thalamic stimulus is separated from that of sensory cortex stimuli in the amygdala (15), (16). In addition, a simple low-pass filter is used for modeling thalamus. The neurophysiological speed response in sensory cortex is faster than in thalamus (14) [14]. Furthermore, auto learning is performed by (15), (16) and (19) in different parts of the controller.

#### IV. DESIGN OF DRIVE CONTROL SYSTEM

As an advanced speed/torque control drive, it should include some features in terms of fast dynamics, independency on parameter variation and simplicity [29]. Since, in SynRM motors, rotor axis synchronously follows that of stator flux, rotor dynamics is affected by stator flux. Therefore, in a transient state, it can be inferred as:

$$\omega_r = \omega_{r0} + \Delta\omega_r \cong \frac{\Delta(\theta_r + \delta)}{T_s}, \quad (25)$$

where  $\omega_{r0}$  and  $\Delta\omega_r$  are primary state and deviation of the rotor speed, respectively. Then, it is resulted in:

$$\Delta\omega_r \cong \frac{\Delta\delta}{T_s}. \quad (26)$$

So, equation (8) is rewritten as:

$$\Delta T_{en} = 2\Delta\lambda_{sn} + 2T_s \cot 2\delta\Delta\omega_r. \quad (27)$$

As discussed above (25)-(27), it means that for driving a deviation on rotor speed, a torque deviation should be applied. But in reality, since the electromagnetic torque dynamic is higher than that of rotor speed, it leads to a restriction on the torque deviation as follows:

$$\Delta T_{en} = \begin{cases} \min(1, 2\Delta\lambda_{sn} + 2T_s \cot 2\delta\Delta\omega_r), & \Delta T_{en} \geq 0 \\ \max(-1, 2\Delta\lambda_{sn} + 2T_s \cot 2\delta\Delta\omega_r), & \Delta T_{en} < 0 \end{cases}. \quad (28)$$

Since normalized deviations should be restricted to a maximum value equal to 1, Eq. (28) is equipped with Max-Min math functions. By using the restriction, the drive system enjoys the whole allowable potential of the electric machine to have maximum dynamic responses. The block diagram of the new control system incorporating the emotional controller (BELBIC) is given in Fig. 3, where speed  $\omega_r$  is controlled by a SDC based on (28), which produces the normalized torque error as an input for TCD (9) where it generates the normalized deviation of  $q$ -axis current reference. The emotional control system receives normalized deviation of the  $q$ -axis and  $d$ -axis component current error signals

corresponding to (21)-(24). It then generates the output signals following (20). As shown in Fig. 3, two emotional intelligent controllers (BELBIC) are employed. The first controller (BELBIC1) has  $q$ -axis torque producing current control responsibility by generating  $v_{qs}^*$  as output, and the second controller (BELBIC2) controls  $d$ -axis current by generating  $v_{ds}^*$  as output. The proposed drive is called SDC-BELBIC in this work. As an advantage, the proposed system can control the machine torque by TDC (9). The control principle is based on flux-oriented control approach in the rotor reference frame. After generating voltage references in the rotor-oriented frame, they are transferred to stationary-reference frame. In order to generate the logic signals to control the inverter switches, the space vector pulse width modulation (SV-PWM) technique is used.

It is evident that a suitable drive control is achieved without any requirement to other conventional controllers (PI, PID controllers, etc.) for speed control and generating command voltages, and quite independent of motor parameters. Unlike conventional PI controllers, the proposed technique enjoys auto learning, parameter-free and the controller coefficients are adaptive, which facilitates FOC control for any electric drives in general. Furthermore, in Fig. 3,  $\theta_s$  is stator flux angle, and  $\delta = \theta_s - \theta_r$ .

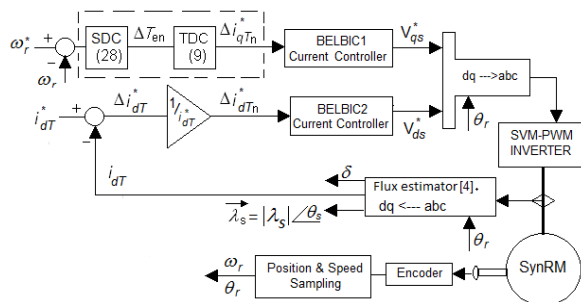


Fig. 3. Block diagram of the control system for SynRM drive.

## V. REAL-TIME EXPERIMENTATION

The block diagram of the proposed system to drive a SynRM, is shown in Fig. 3. In order to evaluate the proposed system in real time conditions, a DSP-based prototype system is built and tested. The experimental setup is presented in Fig. 4, which includes the following parts: a 1.1-kWdc generator as its load and a 0.37-kWthree-phase SynRM, a three-phase voltage source inverter and its isolation board, a voltage source inverter with corresponding driver board, a sensor board, and a TMS320F28335 signal processor board designed by Texas Instrument Co. The switching frequency is selected at 10 kHz for the inverter. Pertinent parameters of the 0.37-kWSynRM are given in the [4]. The saturation of inductances are considered in this study [4], thus having a model with variable parameters.

## VI. DISCUSSIONS AND RESULTS

In order to assess the proposed drive, its performances are

examined by simulation and experimental tests at different conditions. The detailed characteristics of the control system are presented in the Table I. The same tests are performed by using the optimal conventional controller PI (OCC-PI), and the results are compared with those of the purposed SDC-BELBICcontroller. The PI controller is optimally tuned by using a standard genetic algorithm (GA). The  $d$ -axis stator current,  $i_{dT}^*$ , and the speed control closed-loops are optimized under constant conditions of speed=500 rpm and current  $i_{dT}^* = 1A$  simultaneously considering the following cost function  $J$ ,

$$J = \int_{t_1=0}^{t_2} k_w |\Delta\omega_r| + k_i |\Delta i_{dT}^*| dt, \quad (29)$$

where  $k_w, k_i$  are the coefficients of speed and current errors respectively. The propagation and integration coefficients are achieved as (18.5, 16.74) and (7.56, 16.08) for current and speed controllers, respectively. Digital computer simulations are performed by Matlab/Simulink. The simulated responses in Figs.5-8 evaluate the tracking of the system according to the test conditions in Tables II&III. Furthermore, a parameter variation of stator resistance is applied to the system to study the robustness feature at low speed under full load, as shown in Fig.9.

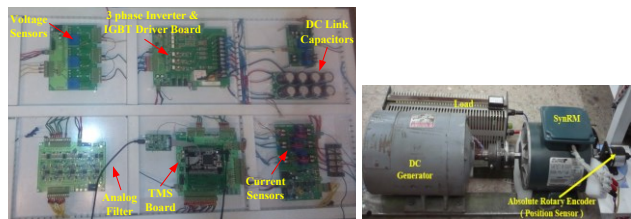


Fig. 4. The experimental setup of the proposed system

TABLE I  
GIN PARAMETERS FOR BELBIC1 AND BELBIC2

$\alpha$	4e-3	$\beta$	30e-3	$K_1$	1
$k_1$	2.1	$k_2$	4	$K_2$	14.5

TABLE II  
THE REFERENCE COMMANDS FOR TEST1, NO LOAD

Time, [s]	0	3	7	10
$\omega_r^*$ [rpm]	500	1000	1000	1000
$i_{ds}^*$ [A]	1	1	1.5	1.5

TABLE III  
THE REFERENCE COMMANDS FOR TEST2.

Time [s]	0	5	9
$\omega_r^*$ [rpm]	1000	1000	1000
$i_{ds}^*$ [A]	1	1	1

Time [s]	0	3.1	6.1	9
$T_L$ [Nm]	0.5	1	0.5	0.5

### A. Simulation and Experimental Results

Fig.5 shows simulation results of the Test1 by using the proposed SDC-BELBIC. As shown, the proposed controller presents regulated responses including small overshoot, fast tracking and zero steady-state error. Considering Fig. 5(a), the actual speed converges to the step command in less than 0.02s with a venial overshoot 0.6%, while steady state error is close to zero as given in Fig. 5(b). Furthermore, the proposed drive system could successfully fulfill the decoupling condition when  $i_{dT}$  tracks a step command at  $t=7s$ .

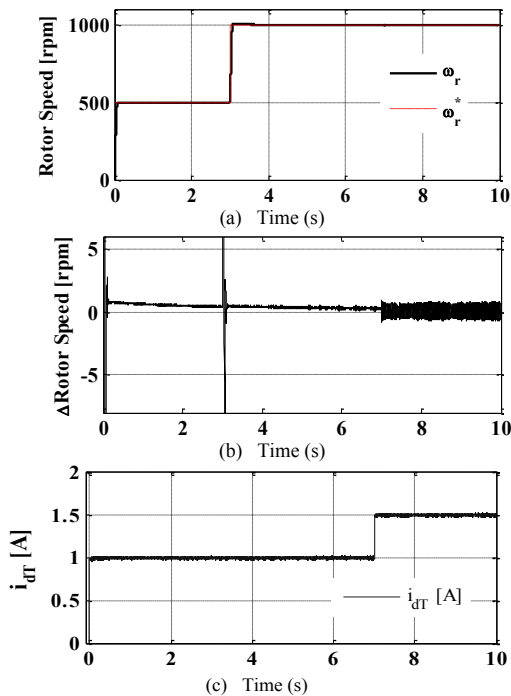


Fig. 5. Simulation results of the SDC-BELBIC, Test1: a) Motor speed response, b) Speed error, c) d-axis stator current component.

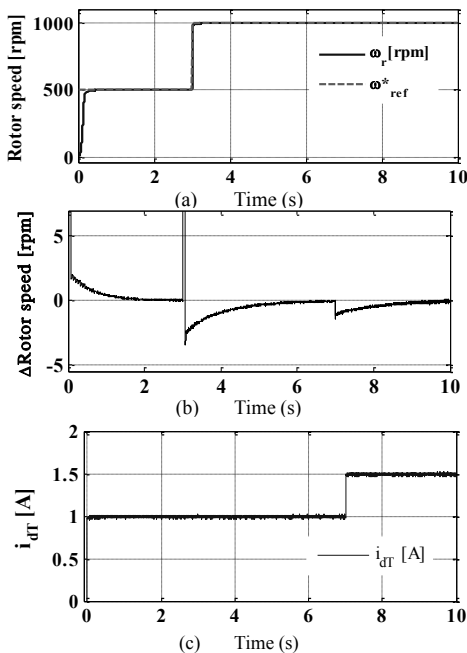


Fig. 6. Simulation results of the OCC-PI, Test1: a) Motor speed response, b) Speed error, c) d-axis stator current component.

On the other hand,  $i_{dT}$  converges to its reference and tracks the command, as given in Fig. 5(c). It could be notable that simultaneous sudden changes in speed and  $i_{dT}$  do not have any permanent impact on the system performance.

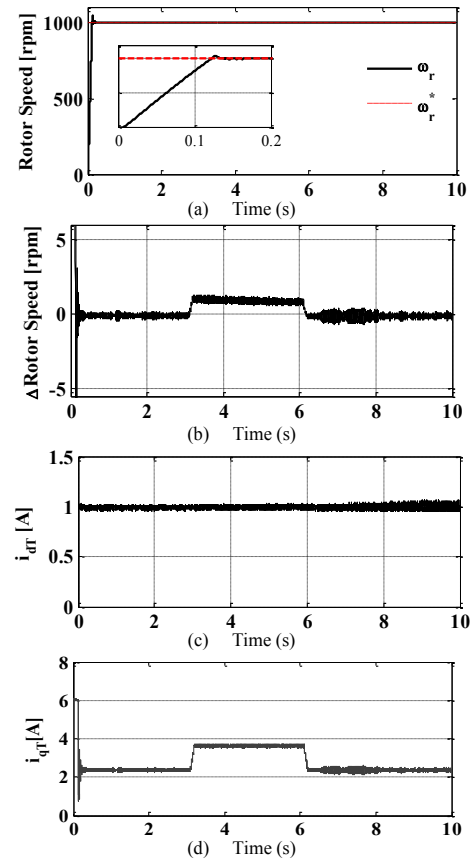


Fig. 7. Simulation results of the SDC-BELBIC, Test2: a) Motor speed response, b) speed error, c, d) dq-axis stator current components.

The achieved results by using OCC-PI are given in Fig. 6. It should be considered here, that the optimal tuning of the PI controllers results in fast dynamics without over/under shoot and minimum error in tracking commands. As it is seen in Figs. 6(a&b), although there is not any considerable error in steady state, its rise time is significant as high as about 0.17s in the first speed step. On the other hand, albeit the time is successfully decreased in the next speed step, it is achieved at the expense of an overshoot and takes a long time to settle at about 1s. In addition, at the step command time for the d-axis stator current component,  $i_{dT}$ , an undershoot is seen with a long settling time of about 1.5s on rotor speed. In other words, the drive system fails to capture decoupling advantages. It is however noted that  $i_{dT}$  adequately follows its reference, as shown in Fig. 6(c). As mentioned, Test1 is done under sudden changes in speed and d-axis current component under no load conditions. For Test2 the speed reference and  $i_{dT}^*$  are presented in Table III under loading conditions. The achieved results of the SDC-BELBIC under Test2 are presented in Fig. 7. The proposed controller shows tuned response including

features of fast tracking without any overshoot and zero steady-state error, while it is under load with sudden changes in load torque. Under the conditions, motor speed has a venial undershoot, which is removed smoothly, as seen in Figs. 7(a&b). Moreover, Figs. 7(c&d) show that  $i_{dT}$  is kept constant on its reference in spite of the variation of the current  $i_{qT}$ .

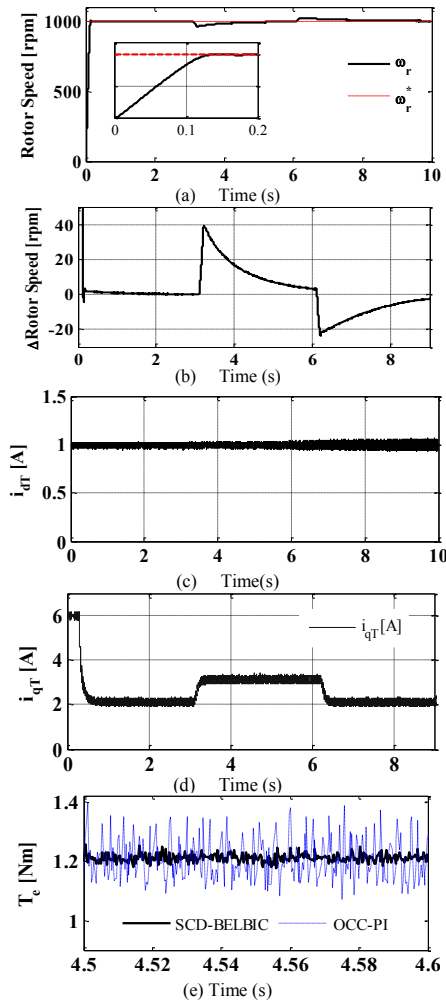


Fig. 8. Simulation results of the OCC-PI, Test2: a) Motor speed response, b) Zoomed speed error, c, d)  $dq$ -axis stator current components, e) steady state of the electromagnetic torque comparing OCC-PI and SDC-BELBIC.

On the other hand, Fig. 8 gives the simulated performance results under Test2 by using the controllers OCC-PI. Albeit Fig. 8(a) shows that OCC-PI has a starting as good as that of the SDC-BELBIC, the actual speed has a very long settling time and a notable under/over shoot under loading conditions, as seen in Fig. 8(b). Also, Fig. 8(c) shows that  $i_{dT}$  could properly converge to its reference. In addition, as presented in Figs. 8(d&e), the torque ripples resulted by  $i_{qT}$  will be higher in comparison with that of the proposed system. Fig. 9 shows the results of low speed test under full loading and stator resistance variation for both OCC-PI and SDC-BELBIC drive systems. While motor is being driven at around a full load of 1.8Nm with speed step of 5 rpm and  $i_{dT} = 1.4$ , the

resistance variation is suddenly applied at  $t=0.2s$ . As shown, OCC-PI fails to capture the imagination and collapses during resistance variation.

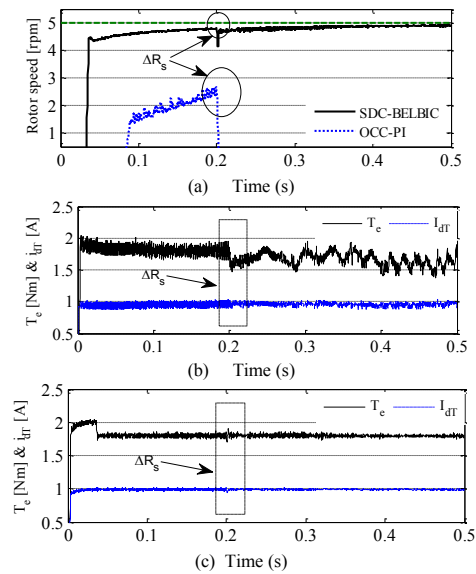


Fig. 9. Simulation results of the low speed test under full load condition; a) rotor speed, b and c) torque and stator current  $i_{dT}$ , by using the OCC-PI, and SDC-BELBIC, respectively.

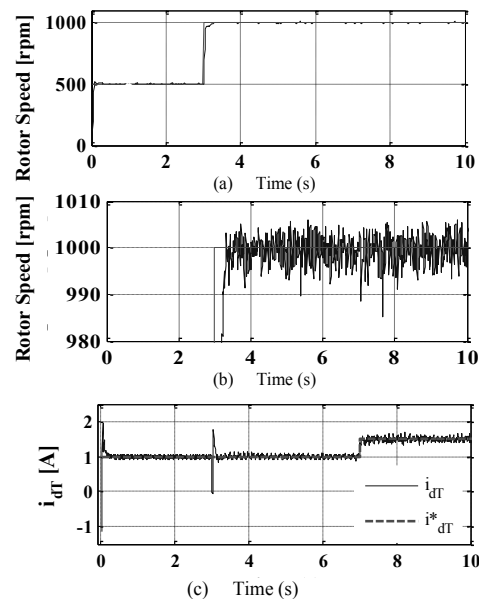


Fig. 10. Experimental results of the SDC-BELBIC, Test1: a) Motor speed response, b) Zoomed speed response, c) d-axis stator current component.

On the other hand, SDC-BELBIC could handle the critical conditions, as shown in Fig.9(a). For OCC-PI method, albeit  $i_{dT}$  is properly controlled on the command line, current controller  $i_{qT}$  could not support the torque after the parameter variation as seen in Fig.9(b). In addition, at normal conditions, although OCC-PI attempts to track its references, it suffers from considerable torque ripples with a very long rise time in comparison with that of SDC-BELBIC, as shown in Figs. 9(b&c).

Experimental tests like those of the simulations are done to verify and evaluate simulated findings. The results under Test1 and Test2 are given in Figs. 10 and 11, respectively. Figs. 10(a&b) indicate the rotor speed and the zoomed speed response within 30 rpm band, and Fig. 10(c) illustrates  $i_{dT}$ , which properly converges to its reference. Fig.11(b) also points to the zoomed experimental speed response at synchronous speed of 1000rpm with a band of 100 rpm. As shown in the Figs. 10 and 11, the obtained experimental results are acceptable, and very similar to those of simulation results in Figs. 5 and 7 respectively. So, the proposed drive system could successfully not only handle the loading conditions without any considerable under/over shoot, as fast as possible, but also satisfy the decoupling circumstance.

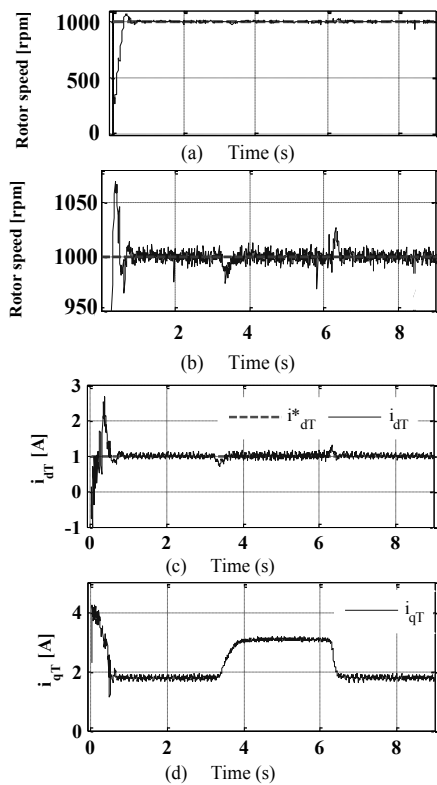


Fig. 11. Experimental results using the SDC-BELBIC, Test 2: a) Motor Speed response, b) Zoomed speed response, c , d)  $dq$ -axis stator current components.

### B. Comments on Results

There exist reasonably close agreements between the simulated and experimental results. By comparing the simulation and experimental test results, it can be reasonably concluded that the enhanced BELBIC can meet the requirements for improved control of the synchronous reluctance motor drives by solving the interior instability caused by the learning process. In addition, by contributing a speed deviation controller, the proposed drive system enjoys advantages of an advanced drive in terms of fast dynamics and robustness against parameter variations, while avoids disadvantages of conventional systems, including PI tuning and dependency on parameters. The robustness raises from the BELBIC and SDC controllers are not dependent on motor

parameters and set points of the operation, while the inductances and stator resistance are varying during operation [4]. SDC-BELBIC could keep its superiority over OCC-PI in different conditions in terms of stability, fast dynamics, low torque ripple, and accuracy. At low speed range, SDC-BELBIC succeeds to reduce the torque ripple up to 20% less than that of OCC-PI, as shown in Figs. 9(b&c).

## VII. CONCLUSION

This paper presented two main contributions, including an enhanced version of the emotional controller in connection with a new normalized speed deviation controller for electrical drives in general. For the first time, simultaneous applying normalization concept and deviation model controller, as speed controller, directly provided a torque deviation signal without any knowledge of motor parameters. In addition, the enhanced BELBIC could overcome the interior instability by modifying learning process in the amygdala, as a challenge of the conventional control. The proposed high performance control method for the synchronous reluctance motor drive not only eliminates the need for conventional PID controllers, but also keeps the system simplicity. A simple and improved structure of brain emotional learning based intelligent controller with its fast auto learning, model-free and good tracking features was used in connection with a new deviation controller based on model but parameter-free. A real-time implementation of the proposed method was represented for a 3-phase SynRM drive. Close agreement was observed between the results of the simulation and the experiment; any discrepancy between them is attributed to the limitations of the data acquisition system. The proposed drive system has adequate insensitivity with respect to system disturbances and parameter variations, particularly in comparison with the optimal-PI controller. The proposed controller system can be easily adapted for high performance industrial applications.

## REFERENCES

- [1] H. Mahmoud and N. Bianchi, "Eccentricity in synchronous reluctance motors-Part I: Analytical and finite-element models," *IEEE Trans. Energy Convers.*, vol. 30, no.2, pp.754-760, Jun. 2015.
- [2] M. Nabil Ibrahim, P. Sergeant, E. Eddin, and M. Rashad, "Combined star-delta windings to improve synchronous reluctance motor performance," *IEEE Trans. Energy Convers.*, vol. 31, no.4, pp.1479-1487, Dec. 2016.
- [3] A. Yousefi-Talouki, P. Pescetto, and G. Pellegrino, "Sensorless direct flux vector control of synchronous reluctance motors including standstill, MTPA, and flux weakening," *IEEE Trans. Ind. Appl.* vol. 53, no.4, pp.3598-3608, 2017.
- [4] E. Daryabeigi, H. Abootorabi Zarchi, Gh. Arab Markadeh, J. Soltani, and F. Blaabjerg, "Online MTPA control approach for synchronous reluctance motor drives based on emotional controller," *IEEE Trans. Power Electron.*, vol. 30, no.4, pp.2157-2166, 2015.
- [5] G. Kenne, T. Ahmed-Ali, F. Lamnabhi-Lagarrigue, and A. Arzande, "Real-time speed and flux adaptive control of induction motors using unknown time-varying rotor resistance and load torque," *IEEE Trans. Energy Convers.*, vol. 24, no.2, pp.375-378, Jun. 2009.
- [6] K. Kai Shyu and C. Keng Lai, "Incremental motion control of SynRM via multi segment sliding mode control method," *IEEE Trans. Cont. Sys. Tech.*, vol.10, pp. 169-176. 2002.
- [7] G. Stumberger, B. Stumberger, and D. Dolinar, "Identification of linear



synchronous reluctance motor parameters," *IEEE Trans. Ind. Applicat.*, vol. 40, no. 5, pp. 1317-1324, 2004.

[8] Q. Liu and K. Hameyer, "High-performance adaptive torque control for an IPMSM with real-time MTPA operation," *IEEE Trans. Energy Convers.*, vol. 32, no. 2, pp. 571-581, Jun. 2017.

[9] C. K. Lin, J. T. Yu, Y. S. Lai, and H. C. Yu, "Improved model-free predictive current control for synchronous reluctance motor drives," *IEEE Trans. Ind. Electron.*, vol. 63, no. 6, pp. 3942-3953, 2016.

[10] H. Hadla and S. Cruz, "Predictive stator flux and load angle control of synchronous reluctance motor drives operating in a wide speed range," *IEEE Trans. Ind. Electron.* vol. 64, no. 9, pp. 6950-6959, Sep. 2017.

[11] X. X. Yin, Y. G. Lin, W. Li, H. W. Liu, and Y. J. Gu, "Fuzzy-logic sliding-mode control strategy for extracting maximum wind power," *IEEE Trans. Energy Convers.*, vol. 30, no. 4, pp. 1267-1287, Dec. 2015.

[12] B. K. Bose, "Neural network applications in power electronics and motor drives-An introduction and perspective," *IEEE Trans. on Ind. Electron.*, vol. 54, pp. 14-33, 2007.

[13] C. Lucas, D. Shahmirzadi, and N. Sheikholeslami, "Introducing BELBIC: brain emotional learning based intelligent control," *International Journal of Intelligent Automation and Soft Computing*, vol. 10, pp. 11-22, 2004.

[14] C. Lucas, "BELBIC and its industrial applications: towards embedded neuroemotional control codesign," *Springer, Integrated Systems, Design and Technology, Part 3*, pp. 203-214, 2011

[15] M. R. Jamali, M. Dehyadegari, A. Arami, C. Lucas, and Z. Navabi, "Real-time embedded emotional controller," *J. Neural Comput & Applic*, Springer-Verlag London, vol. 19, no. 1, pp. 13-19, 2010.

[16] M. A. Sharbafi, C. Lucas, and R. Daneshvar, "Motion control of omnidirectional three-wheel robots by brain-emotional-learning-based intelligent controller," *IEEE Trans. Sys. MAN, & Cyber-Part C: Applic. & Reviews*, vol. 40, pp. 630-638, 2010.

[17] M. Hosseinzadeh Soreshjani, Gh. Arab Markadeh, E. Daryabeigi, N. Reza Abjadi, and A. Kargar, "Application of brain emotional learning-based intelligent controller to power flow control with thyristor-controlled series capacitance," *IET Generation, Transmission & Distribution*, vol. 9, no. 14, pp. 1964-1976, 2015.

[18] E. Daryabeigi, Gh. Arab Markadeh, and C. Lucas, "Emotional controller in electric drives-A review," *36th Annual Conference on IEEE Industrial Electronics Society (IECON)*, 2010, pp. 7-10.

[19] M. A. Rahman, R. M. Milasi, C. Lucas, B. N. Arrabi, and T. S. Radwan, "Implementation of emotional controller for interior permanent magnet synchronous motor drive," *IEEE Trans. Ind. Applicat.*, vol. 44, pp. 1466-1476, 2008.

[20] B. Mirzaei Dehkordi, A. Kiyomarsi, P. Hamedani, and C. Lucas, "A comparative study of various intelligent based controllers for speed control of IPMSM drives in the field-weakening region," *Expert Systems with Applications*, vol. 38, pp. 12643-12653, 2011.

[21] E. Daryabeigi, H. Abootorabi Zarchi, Gh. R. Arab Markadeh, M. A. Rahman, and C. Lucas, "Implementation of emotional controller (BELBIC) for synchronous reluctance motor drive", in *Proc. IEEE, IEMDC, Agu. 2011*, pp. 1088-1093.

[22] M. Masoudinejad, R. Khorsandi, A. Fatehi, C. Lucas, S. Fakhimi Derakhshan, and M. R. Jamali, "Real-time level plant control using improved," *BELBIC. IFAC Conf. Proc.*, 2008, pp. 4631-4635.

[23] S. A. Nahian, D. Q. Truong, and K. K. Ahn, "A self-tuning brain emotional learning-based intelligent controller for trajectory tracking of electrohydraulic actuator," *Proceedings of the Institution of Mechanical Engineers, Part I: J. Systems and Control Engineering*, vol. 228, no. 7, 2014, pp. 461-475.

[24] P. Struss, "Deviation models revisited," In *Working Papers of the 18th International Workshop on Qualitative Reasoning*, 2004.

[25] E. Daryabeigi and S. Vaez-Zadeh, "A combined control for fast and smooth performance of IPM motor drives over wide operating conditions," *IEEE Trans. Energy Conversion*, vol. PP, no. 99, pp. 1-1, 2018.

[26] R. P. Aguilera, P. Lezana, and D. E. Quevedo, "Finite-control-set model predictive control with improved steady-state performance," *IEEE Trans. Indus. Inf.*, vol. 9, no. 2, pp. 658-667, 2013.

[27] S. Vaez-Zadeh, "Control of permanent magnet synchronous motors," Oxford university press, Oxford, 2018.

[28] H. Abootorabi Zarchi, Gh. Arab Markadeh, and J. Soltani, "Direct torque and flux regulation of synchronous reluctance motor drives based on input-output feedback linearization," *Energy Conversion and Management*, vol. 51, Issue 1, pp. 71-80, 2010.

[29] S. Vaez-Zadeh, "Analysis of a DTC with back EMF oriented voltage for PMS motor drives," *IEEE Transactions on Energy Conversion*, early access, 2018.



**Ehsan Daryabeigi** received the B.Sc. degree from the Islamic Azad University (IAU), Yazd, Iran, in 2005 and the M.Sc. degree from the IAU, Najafabad, Iran, in 2009, all in electrical engineering. He is currently working toward the PhD degree in Yazd University Yazd, Iran. He has been an Associate Researcher with the Advanced Motion Systems Research Laboratory, University of Tehran, Tehran, Iran, since 2011.



**Ahmad Mirzaei** received the B.S. degree in 1988, M.S. degree in 1994 and the Ph.D. degree in power engineering from Isfahan University of Technology, Isfahan, Iran, in 2005. He is an Assistant Professor at Yazd University, Yazd, Iran. His research interests include power systems, electrical machines, electric power quality and intelligent systems, He is the Director of the Electric Power Quality and Intelligent Systems Laboratory.



**Hossein Abootorabi Zarchi** received the M.S. and Ph.D. degrees from the Isfahan University of Technology, Isfahan, Iran, in 2004 and 2010, respectively. He was a Visiting Ph.D. Student with the Control and Automation Group, Denmark Technical University, Denmark, from May 2009 to February 2010. He is currently an Assistant Professor in the Department of Electrical Engineering, Ferdowsi University of Mashhad, Mashhad, Iran.



**Sadeh Vaez-Zadeh** (S'95-A'03-SM'05) received the B.S. degree from the Iran University of Science and Technology, Tehran, Iran, in 1985 and the M.S. and Ph.D. degrees from Queen's University, Canada, in 1993 and 1997, respectively, all in electrical engineering. He has been a Full Professor at the University of Tehran, since 2005. Dr. Vaez-Zadeh is an Editor of the *IEEE TRANSACTIONS ON ENERGY CONVERSION* and a Subject Editor of the *IET RENEWABLE POWER GENERATION*.